Atom Indonesia

Journal homepage: https://atomindonesia.brin.go.id

Characterization and Sorption Study of Cesium-137 by Bentonite from Santrijaya, Indonesia as an Engineering Barrier Material for Radioactive Waste Disposal Facilities

H. Sriwahyuni[1,2,*], Y. K. Krisnandi[1*], T. Basuki[2], B. Setiawan[2], A. Budianti[3], Z. Anggraini[2], G. Nurliati[2], N. S. Pamungkas[2,4]

[1]*Departement of Chemistry, Faculty of Mathematics and Natural Sciences, Universitas Indonesia, Depok 16424, Indonesia*
[2]*Research Center for Nuclear Material and Radioactive Waste Technology (PRTBNLR), National Research and Innovation Agency, KST BJ.Habibie, South Tangerang 15314, Indonesia*
[3]*Directorate of Nuclear Facilities Management, National Research and Innovation Agency, KST BJ. Habibie, South Tangerang 15314, Indonesia*
[4]*Radionuke Consultant Indonesia, Pati 59113, Indonesia*

ARTICLE INFO

Article history:
Received 6 February 2025
Received in revised form 17 June 2025
Accepted 23 June 2025

Keywords:

Sorption
Cesium
Bentonite
Engineered barrier
Disposal facilities
Radioactive waste

ABSTRACT

Engineered barrier materials, such as bentonite, play a critical role for the safety of radioactive waste disposal systems by limiting radionuclide migration. This study aims to evaluate the mineralogical, chemical, and morphological characteristics of natural bentonite from Santrijaya, Tasikmalaya, Indonesia, and to investigate its Cs-137 sorption behavior, focusing on its potential as a candidate for engineered barrier materials. X-Ray Diffraction (XRD) and X-Ray Fluorescence (XRF) analyses showed that the bentonite predominantly consists of montmorillonite, with silica contributing about 80 percent of its composition. The material shows a specific surface area of 121.89 m²/g and a cation exchange capacity of 43.23 meq/100g, supporting its suitability for radionuclide sorption. The sorption capacity at equilibrium (q_e) achieved at 536.67 mg-Cesium/g-bentonite after 10 days of contact time, with adsorption kinetics that follows the Pseudo-Second Order (PSO) model and the distribution coefficient (K_d) value of 5211 mL/g. The study shows the competitive effects of K^+ and Na^+ ions, with K^+ ions showing a stronger competitiveness for Cs-137 binding sites than that of Na^+, which could influence radionuclide retention. These findings highlight the high sorption efficiency and stability of Santrijaya bentonite, showing its potential as a barrier material for radioactive waste containment systems and suggest the necessity of considering competing ion interactions in the design of barrier materials.

INTRODUCTION

Radioactive waste is a byproduct of the use of nuclear technology applications in various fields, including energy generation [1,2], medical utilization [3], and laboratory experiments [4]. As these technologies continue to advance, the management of radioactive waste becomes increasingly critical. Radioactive waste poses long-term risks to both the environment and human health due to its hazardous nature and prolonged radioactive decay periods [5,6]. Improper management could result in irreversible environmental damage and public health issues, creating a legacy that burdens future generations [7]. Therefore, the safe disposal of radioactive waste is essential, and its management requires careful planning and execution to mitigate potential risks [8,9].

The safety of radioactive waste disposal requires effective barriers, a stable location, and strict monitoring. Studies show that Cs-137 might migrate in the sediments, enter the food chain, and increase radiation exposure. As a result, disposal facilities must be designed to avoid contamination and protect the environment and human health [10-12].

In Indonesia, processed radioactive waste is primarily stored in temporary storage sites, which will subsequently be permanently stored in a

*Corresponding author.
E-mail address: yuni.krisnandi@sci.ui.ac.id
DOI: https://doi.org/10.55981/aij.2025.1628

sustainable storage facility for radioactive waste disposal. In radioactive waste disposal facilities, one important component in disposal systems is an engineered barrier system designed to prevent the release of radionuclides into the environment [13,14]. An engineered barrier system plays a role in slowing down the movement of radionuclides stored in the disposal facility into the environment. Moreover, it ensures radionuclides remain contained in the long term. Bentonite, a natural clay material, is widely recognized as a potential engineered barrier material in the safety system of radioactive waste disposal facilities due to its unique physicochemical properties [15-17]. The engineered barrier for radioactive waste disposal facilities must be able to withstand radiation, absorb radionuclides, prevent water ingress, and be mechanically stable in the long term. The barrier must also comply with nuclear safety and geological standards [18,19]. Bentonite has properties that support the function of engineered barrier materials. Its high swelling ability facilitates gap closure [20], low permeability prevents water loss, high sorption capacity enables radioactive absorption, and self-sealing properties enhance safety and protection effectiveness [21-23].

Research on the ability of bentonite to absorb radionuclides has been conducted, particularly regarding its role as an engineered barrier in radioactive waste disposal facilities. The prior study results showed that bentonite can also absorb Strontium-90 (Sr-90) with a K_d of 13,700 mL/g, measured through contact between bentonite (from Bogor and Padang) and radionuclides over a certain period. The results revealed that changes in ionic strength and the initial concentration of Sr-90 in the solution significantly affect the absorption of Sr-90 in the bentonite samples [24]. Moreover, a study by Purnomo (2010) reported that bentonite from Yogyakarta was less efficient in absorbing Sr-90 due to the presence of competitive ions such as Mg^{2+}, K^{+}, Na^{+}, and Ca^{2+} [25].

Further research has also explored the sorption study of Cs-137 by bentonite globally. A study on cesium sorption has been conducted using bentonite and silty clay from Iran. The research results showed that bentonite (253.98 L/kg) concluded a higher cesium absorption capacity compared to silty clay (213.65 L/kg) [26]. Other research reports (bentonite from Cherkasy, Ukraine) revealed significant capability in capturing Cs-137, with a sorption efficiency reaching 85%. This sorption process reached equilibrium conditions within 10-12 hours, where bentonite achieved its maximum absorption level for Cs-137 [27]. In addition, an experiment utilizing bentonite from Russia by Belousov et al. (2019) discovered that sodium-type bentonite succeeded Cs-137 sorption with a capacity of 0.55 μmol/g [28].

The selection of Santrijaya bentonite was strategically based on several factors, primarily its geographical proximity to the proposed radioactive waste disposal site in Serpong, South Tangerang [29]. This advantageous location significantly reduces transportation time and costs while ensuring consistent material availability. To support the development of a new permanent radioactive waste disposal facility, which will include handling Cesium-137 (Cs-137) with a half-life of 30 years, this study aims to evaluate the characteristics and sorption capacity of bentonite from Santrijaya in Cs-137 radionuclide. There has never been any research done on Santrijaya bentonite as a designed engineered barrier system for the disposal of radioactive waste. As a result, this assessment takes into account its possible application as an engineered barrier material for the containment of radioactive waste. The findings of this research will help develop efficient methods for the final storage of radioactive waste that prioritize public safety and environmental preservation.

METHODOLOGY

Materials

The materials used in this study were bentonite from Santrijaya, West Java, Indonesia, and chemicals produced by Merck: Cesium Chloride (CsCl, pro analysis CAS number: 7647-17-8), Potassium Chloride (KCl, pro analysis CAS number: 7447-40-7), Sodium Chloride (NaCl, pro analysis CAS number: 7647-14-5), Cesium-137 radioactive solution 23.14 Bq (A_0) of activity from Eckert and Ziegler Isotope Production as a tracer stock, and demineralized water.

Methods

Material collection and characterization

Bentonite samples were collected from the Santrijaya area, Tasikmalaya (denoted as Santrijaya bentonite). The obtained samples were then sieved to the particle size range of 80 to 200 mesh using a Fritsch Gmbh Brd-6580 sieve. Phase characterization of the sample was performed using an X-Ray Diffraction (XRD) instrument with a PANalytical AERIS (Cu-Kα source) in the 2θ range from 5° to 85°. To analyze the chemical composition, X-Ray Fluorescence (XRF) ARL Quant'X was used at a temperature of 20.5 °C and a relative humidity of 50%. The functional groups of

bentonites were observed using Fourier Transform Infrared Spectroscopy Middle Infrared Region-Attenuated Total Reflectance (FTIR MIR-ATR), with a measurement wavelength range from 500 to 4000 cm^{-1}. The surface morphology of the samples was studied using SEM-EDS JEOL-JSM6510LA with magnifications of 750× and 1500×. The cation exchange capacity was analyzed in the TekMira laboratory, while the Specific Surface Area (SSA) of the samples was measured using the NOVAtouchTM 2LX SSA analyzer and the Brunauer-Emmett-Teller (BET) method.

Sorption and kinetic studies

The sorption experiment was conducted by contacting the sample (0.1 g) with 10 mL Cs-137/CsCl mixture solution (A_0: 23,140 Bq/250 mL, CsCl 10^{-8} M) for 1 to 28 days; then, the liquid and solid phases were separated using a Heraeus Labofuge 400 centrifuge for 10 minutes at a speed of 2500 rpm. The liquid phase was analyzed using a high-purity Germanium (HPGe) gamma radiation detector and a Multichannel Analyzer (MCA) to determine the Cs-137 activity at an energy level of 662 keV. The results of Cs-137 concentrations in the initial and final analyses were used to calculate the adsorbed amount of Cs-137 at the time t value as the final concentration of cesium as (mg/g) (q_t). Eq. (1) was used to calculate the q_t value from the experimental data [30,31].

$$q_t = (C_0 - C_t) \times \frac{V}{m} \quad (1)$$

Where q_t, C_0, C_t, V, and m are the adsorbed amount of Cs-137 (mg-Cs/g-bentonite), the initial concentration of Cs-137 (mg/L), the final concentration of Cs-137 (mg/L), the total volume of solution (mL), and the dry mass of the sample (g), respectively.

The mechanism of Cs-137 sorption on bentonite surfaces was performed using the experimental data from the variation of reaction time. The performance is based on the application of two common kinetic sorption linearized models, such as pseudo-first-order (PFO) and pseudo-second-order (PSO), which are written by Eqs. (2) and (3), respectively [32-34].

Pseudo-First-Order Model (PFO). The Lagergren first-order kinetic model assumes the adsorption rate is proportional to the difference between the equilibrium concentration ($q_e; mg/g$) and the adsorbed concentration at the time t ($Q_t; mg/g$). The linear form equation for PFO Eq. (2) was provided as follows:

$$ln(q_e - q_t) = lnq_e - k_1 t \quad (2)$$

where k_1 (min^{-1}) is the PFO rate constant.

Data is plotted according to different kinetic models to analyze adsorption kinetics to extract key parameters such as rate constants and equilibrium adsorption capacity ($q_e; mg/g$). For the PFO model, Eq. (2) is used. Experimental values ($ln\,(q_e - q_t)$) are plotted versus time ($t; minutes$), provided in a linear relationship. The slope of the line informs the rate constant (k_1), and the y-intercept gives lnQ_e.

Pseudo-Second-Order Model (PSO). This model assumes that adsorption involves chemisorption and that the rate depends on the squares of the unoccupied sites. The linear form equation for PSO Eq. (3) was given as follows:

$$\frac{t}{q_t} = \frac{1}{k_2 q_e^2} + \frac{1}{q_e} t \quad (3)$$

where k_2 (g / (mg·min)) is the PSO rate constant.

For the PSO model, Eq. (3) is utilized. A graphic of $\frac{t}{Q_t}$ versus t gives a linear relationship, where the slope and intercept are used to calculate Q_e, and the rate constant k_2.

Distribution coefficient study

The distribution coefficient is determined using the following formula Eq. (4) [32,35]:

$$K_d = \frac{[Cs\ ions]_{solid}}{[Cs\ ions]_{liquid}} \quad (4)$$

Where K_d is the sorption coefficient of Cs-137 (L/kg), $[Cs\ ions]_{solid}$ is the concentration of Cs-137 in the solid phase (Bq/g), and $[Cs\ ions]_{liquid}$ is the concentration of Cs-137 in the aqueous phase (Bq/mL).

RESULTS AND DISCUSSION

Mineralogical analysis

The Santrijaya bentonite sample's mineralogical profile was characterized using XRD in the 2θ angle range from 5° to 80° as depicted in Fig. 1. XRD spectrum showed a major peak of montmorillonite $(Na,Ca)_{0.33}(Al,Mg)_2(Si_4O_{10})(OH)_2{\cdot}nH_2O$ as the dominant phase in the structure of Santrijaya bentonite. Montmorillonite is the main constituent mineral in bentonite, which has a high silica content [36]. The presence of other minerals such as quartz (SiO_2), kaolinite ($Al_2Si_2O_5(OH)_4$), and clinoptilolite $(Na,K,Ca)_2\text{-}3Al_3(Al,Si)_2Si_{13}O_{36}{\cdot}12H_2O$ further strengthens the character of bentonite, which is rich in silica elements [37].

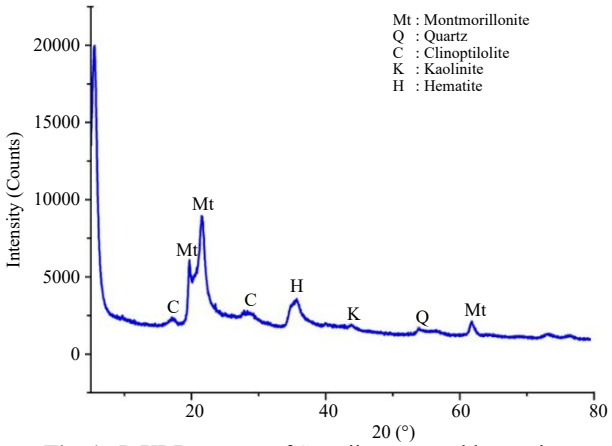

Fig. 1. P-XRD spectra of Santrijaya natural bentonite.

Meanwhile, the mineral hematite indicates the presence of the Fe element in Santrijaya Bentonite, as captured in the spectrum at 2θ around 35.79° [38]. The findings in this study are consistent with the diffraction pattern of bentonite in previous research, where XRD analysis results indicate that the bentonite contains montmorillonite, clinoptilolite, kaolinite, and quartz minerals [39].

Elemental analysis

The elemental results obtained using XRF analysis are listed in Table 1, which informs the elemental composition of Santrijaya bentonite. Based on Table 1, Santrijaya bentonite is a type of calcium bentonite with a calcium (Ca) content of 4.61%. The high silica (Si) content specifies that Santrijaya bentonite has a strong silicate structure in the tetrahedral layer, which affects its cation exchange capacity and good sorption ability [40]. The very high silica content in the XRF results (82.22%) supports the presence of silicate mineral phases such as montmorillonite and quartz, which were identified through XRD as the main phases in the bentonite. The significant iron content (10.65%) from the XRF results can be explained by the presence of hematite observed in the XRD results.

Table 1. Elemental composition of Santrijaya bentonite based on XRF analysis.

Element	Mol (%)
Si	82.22
K	0.93
Ca	4.61
Ti	0.78
Fe	10.65
Sr	0.41
Zr	0.25
Al	14.06

Meanwhile, minor elements such as potassium, strontium, and zirconium, present in small amounts, still influence the physical and chemical properties of the bentonite [41].

Morphology profiles

The provided SEM images in Fig. 2 illustrate the surface morphology of bentonite at two different magnifications: 750× and 1,500×. At 750× magnification, the SEM image offers a broader view of the bentonite surface, revealing a heterogeneous size with particles appearing in varying shapes and sizes. In contrast, the 1,500× magnification image provides a more detailed view, clearly defining the particles and showing intricate details of the particle size. The higher magnification highlights finer details, such as smaller particle clusters and more defined surface textures, with a more compact arrangement of particles compared to the lower magnification. The irregular, aggregated lamellar particles shown in SEM pictures (Fig. 2) are consistent with the usual morphology of smectite clay. However, BET analysis is necessary for quantifying surface area and nanoporosity.

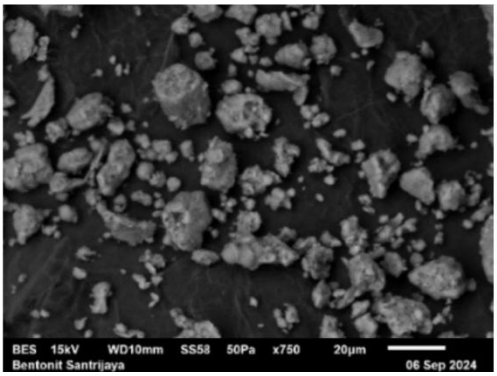

(a)

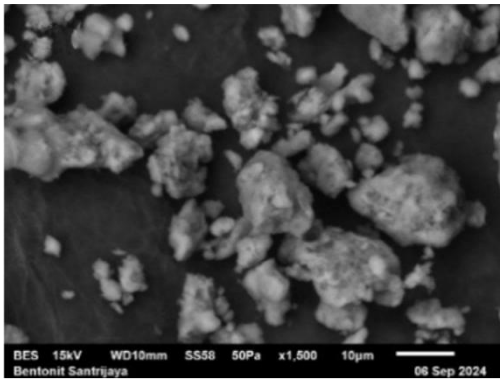

(b)

Fig. 2. Surface morphology of bentonite Santrijaya at magnifications of (a) 750× and (b) 1,500×.

Specific Surface Area (SSA) analysis

Based on the isotherm profile from SSA analysis using the BET (Brunauer-Emmett-Teller) method in Fig. 3, it can be seen that the amount of N_2 gas adsorbed on the bentonite increases with the increase in relative pressure, and the sharp increase after P/P_0=0.4 is caused by capillary condensation within the mesopores categorized as isotherm IV models by International Union of Pure and Applied Chemistry (IUPAC) [42-44].

This hysteresis indicates that the desorption process does not occur directly, as gas is trapped within the pores and released at low pressure, associated with the cylindrical pores of bentonite [45].

From characterization using an SSA analyzer, it was found that Santrijaya bentonite has a specific surface area of 121.889 m^2/g, with an average pore radius of 3.51 nm, indicating that Santrijaya bentonite falls into the mesoporous material category. The larger the surface area, the more area is available for interaction with gas or liquid molecules, which can enhance its sorption capacity [46]. According to studies by Fisli et al., Sukabumi bentonite has a surface area of 77.26 m^2/g and a particle size of 2.17 µm [47]. Compared to the other local bentonites from Indonesia, Santrijaya bentonite has a specific surface area better than Sukabumi bentonite.

Functional group analysis

Figure 4 depicts the FT-IR spectra of some characteristics of the bentonite Santrijaya and the Cs-bentonite Santrijaya peaks. On comparing the transmission peaks of both peaks, a broad band observed from 3500 to 3300 cm^{-1} corresponds to O-H stretching vibrations, which are characteristic of hydroxyl groups from water vapour on the bentonite surface [48,49]. Around 1600 cm^{-1}, a band associated with H-O-H bending vibrations of adsorbed water is prominent in both spectra [50]. The strong peak near 1030 cm^{-1}, attributed to Si-O stretching vibrations from the silicate layers, remains present before and after sorption. A bending vibration at 625 cm^{-1} is associated with Si-O groups [51]. Furthermore, an apparent IR spectrum is observed at 2410 cm^{-1} after Cs adsorption that is probably attributed to the attached CO_2 from the ambient atmosphere [52]. In addition, the IR spectrum around 2000 - 3000 cm^{-1} is not characteristic of bentonite IR spectra that could be from impurities such as iron oxide [53], by considering the P-XRD and XRF analysis results that show a substantial amount of hematite in the sample (Fig. 1, Table 1). This slight spectral change before and after cesium sorption suggested that FTIR analysis was less effective in identifying the cesium on bentonite, as it aligns with the prior study of cesium ions sorption on chitosan [54].

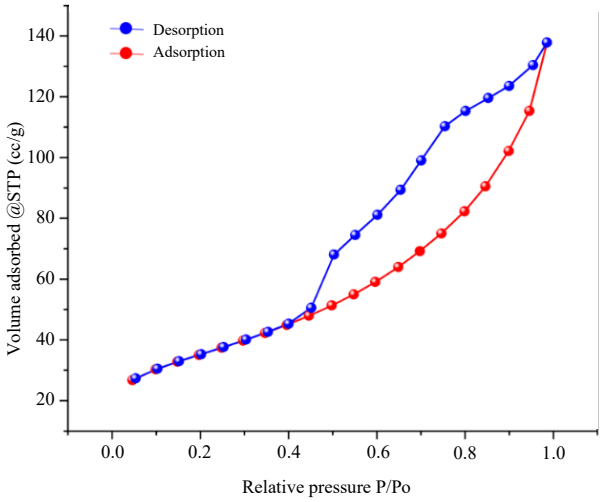

Fig. 3. N_2 adsorption isotherm profile of Santrijaya bentonite.

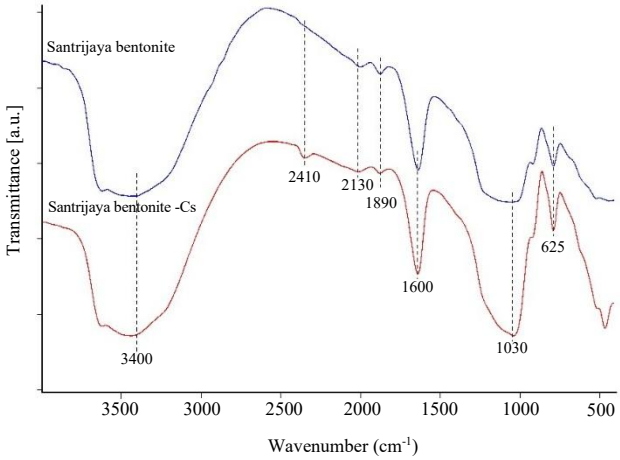

Fig. 4. FTIR spectra of Santrijaya bentonite before and after the sorption study.

Cesium-137 sorption performance

Cesium-137 sorption and kinetic studies

The results of the Cs-137 sorption experiment by the Santrijaya bentonite generally showed that the adsorbed amount of Cs-137 (q_t,) value increased with the increase in contact time, as depicted in Fig. 5. In the early stages, cesium adsorption progressed rapidly during the first 100 hours due to the high availability of active sites on bentonite. As adsorption sites became saturated with Cs-137 over time, the process slowed and moved toward a state of equilibrium. From Fig. 5, the longer the contact time, the more efficiently Santrijaya bentonite absorbed Cs-137 from the solution. After approximately 14,400 minutes or 10 days, an equilibrium state is observed when the result is observed at 510 mg-Cesium/g-bentonite. Equilibrium conditions occur because the active site of bentonite has reached a saturation level.

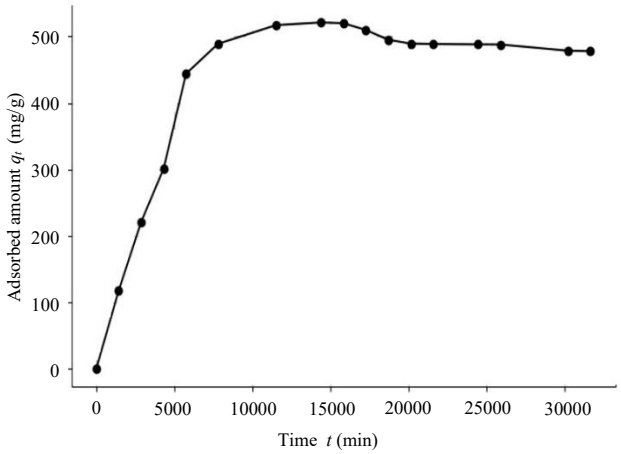

Fig. 5. Adsorption kinetics of Cs-137 by Santrijaya bentonite.

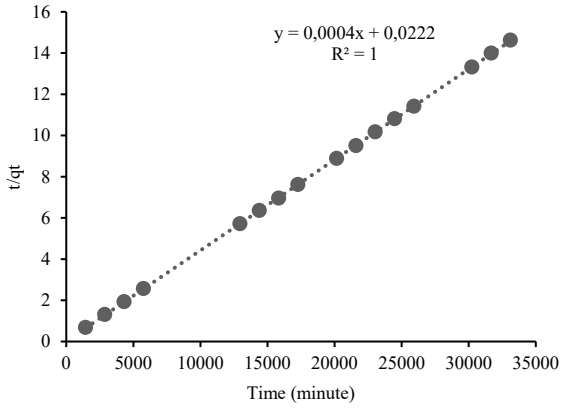

(a)

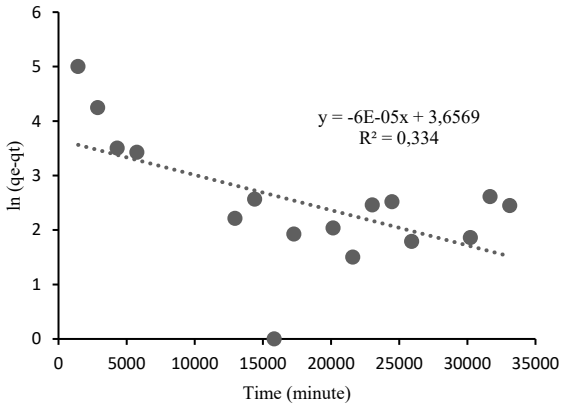

(b)

Fig. 6. Kinetics fitting plot of Cs-137 adsorption by Santrijaya bentonite using PSO (a) and PFO (b) models.

Table 2. Kinetics study parameters of Cs-137 adsorption by Santrijaya bentonite.

Kinetic model	Parameters	Result
PSO	k_2 (g/mg.min)	7.2072
	$q_{e,exp}$ (mg/g)	2500
	R^2	1
	h	0.0222

The provided data in Fig. 6 and Table 2 presented the outcomes of PFO and PSO analysis for the sorption of cesium on Santrijaya bentonite. Based on the fitting results, the higher squared-R (R^2 PSO = 1) suggests that the adsorption followed the PSO model. This indicates that the mechanism is most likely controlled by chemical adsorption (chemisorption). This finding is in agreement with prior studies by Zhang et al. [55], Prajitno et al. [56], and Muslim et al. [57]. This insight emphasizes the importance of chemical bonding in the adsorption of cesium onto bentonite clay, where Cs-137 adsorption on bentonite is a process controlled by surface chemical reactions based on ion exchange and occurs rapidly, consistent with the characteristics of the pseudo-second-order model commonly used to describe adsorption processes based on specific chemical interactions. The bentonite has active sites that can interact with Cs in solution, and the reaction rate is determined by the availability of active sites in the structure of the bentonite, leading to increased sorption capacity.

According to earlier studies [58], Ca-bentonite under saline and alkaline conditions demonstrated a high match with the PSO model (R^2 = 0.99), with ion exchange and the development of secondary minerals such as zeolites influencing Cs retention and boosting adsorption capacity. The PSO model continues to be the most effective way to describe the sorption kinetics, suggesting that improved chemical interactions on the bentonite surface contribute to higher adsorption efficiency. In another study, bentonite was modified with vanadium molybdate, increasing the sorption capacity to 26.72 mg/g in comparison to regular bentonite (18.92 mg/g), with the PSO model being the best way to show the sorption kinetics, it is clear that improved chemical interactions on the bentonite surface support the higher adsorption efficiency [59].

Ion strength study (the presence of Na^+ and K^+ ions)

In Fig. 7, it can be seen that the K^+ ion has a greater influence compared to the Na^+ ion in the process of Cs-137 adsorption by Santrijaya bentonite. In high concentrations of K^+ ions (KCl), the K_d value decreases, which is caused by most of the active sites in bentonite being occupied by K^+ ions, making bentonite less effective in capturing Cs-137. Similarly, in a high concentration of Na^+ ions (NaCl), bentonite can still engross Cs-137, but the effect is smaller compared to K^+ ions. From this finding, it can be concluded that the presence of K^+ ions has a greater influence than the presence of Na^+ ions in the Cs-137 sorption mechanism by Santrijaya bentonite. This is because K^+ ions have lower hydration energy, making it easier to release water molecules and interact with the bentonite surface compared to Na^+ [60].

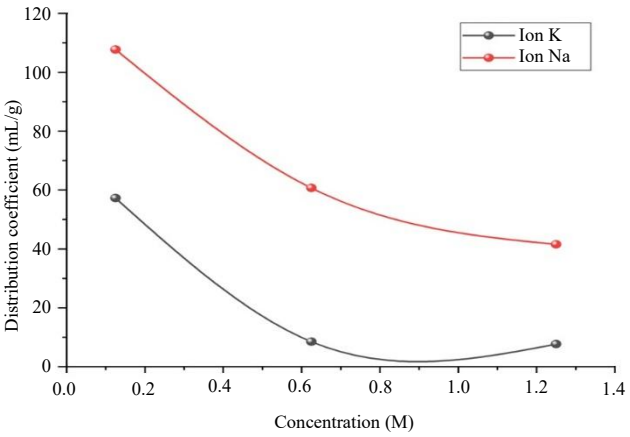

Fig. 7. Effect of ion strength on Cs-137 adsorption by Santrijaya bentonite.

The effect of CsCl concentration on Cs-137 sorption

Based on Fig. 8, the effect of stable CsCl (natural cesium) concentration on the adsorption of Cs-137 by Santrijaya bentonite can be explained. The higher the CsCl concentration, the weaker the ability of bentonite to adsorb Cs-137. At a CsCl concentration of 10^{-7} M, the K_d value is 3,401 mL/g, which means bentonite is effective in capturing Cs-137 because the number of Cs^+ ions in the solution is still low, allowing bentonite to easily adsorb Cs-137. However, as the CsCl concentration increases, the K_d value decreases. This is because the more Cs^+ ions in the solution, the fewer active sites for the absorption of Cs-137 in bentonite, resulting in decreased absorption capacity of Cs-137 by bentonite [60].

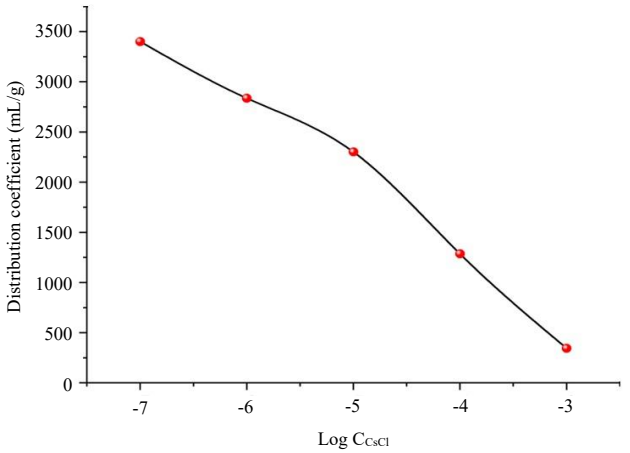

Fig. 8. Effect of CsCl concentration on Cs-137 sorption by Santrijaya bentonite.

Cation Exchange Capacity (CEC)

Cation Exchange Capacity (CEC) is the total number of cations that can be exchanged on the negatively charged colloid surface and is an indicator of the ability of bentonite to adsorb and exchange cations from the solution. A high CEC indicates the effectiveness of bentonite as an adsorbent [61]. The Cation Exchange Capacity (CEC) analysis of Santrijaya bentonite yielded a result of 43.23 meq/100g, which is equivalent to 43.23 mmol of Cs^+ per 100 g of bentonite. The comparison between the CEC value and the sorption data for Santrijaya bentonite reveals significant insights into its adsorption behavior. With a CEC of 0.4323 mmol/g, the material's capacity for cation exchange is notably lower than its measured maximum sorption capacity qm of 3.73 mmol/g (495.66 mg-Cs/g-bentonite), and the distribution coefficient K_d equivalent to approximately 39.19 mmol/g (5211 mL/g). The K_d-derived sorption is nearly 91 times higher than the CEC, indicating that cesium adsorption is not solely governed by cation exchange. Instead, other mechanisms, such as surface complexation, pore filling, or precipitation, significantly contribute to the overall sorption process. This suggests that Santrijaya bentonite has a strong affinity for cesium ions, making it highly effective for adsorption applications beyond what is predicted by its CEC alone [28].

CONCLUSION

In summary, Santrijaya bentonite is dominated by the montmorillonite phase with a high silica content (82.22%) in the mineralogical analysis by XRD and XRF instruments. Morphological analysis using SEM-EDS showed a heterogeneous surface with particles of diverse sizes and shapes. Physical characterization revealed a specific surface area of 121.889 m²/g, a mesoporous structure with an average pore radius of 3.5074 nm. The functional group information, before and after the sorption process, revealed from FTIR analysis, confirmed the involvement of -OH, Si-OH, and -O-Si/-O-Al groups in Cs-137 sorption via complexation mechanisms. The kinetic sorption study confirmed that the PSO model fit very well through the experimental data, indicating chemisorption as the dominant process. The maximum distribution coefficient (K_d) was 5,211 mL/g after 240 hours, with competitive ion studies showing that K^+ ions significantly reduced Cs-137 sorption compared to Na^+ ions. The experimental sorption capacity value was observed to be higher than CEC

43.23 meq/100g. Moreover, the presence of natural cesium ions influences the Cs-137 sorption process. These findings validate Santrijaya bentonite's suitability as a barrier material for radioactive waste disposal, highlighting its high sorption efficiency and structural stability in radioactive waste containment systems. Additionally, future research could explore its performance under varying environmental conditions to further support its application in engineered barrier systems for long-term applications.

ACKNOWLEDGMENT

The authors acknowledge the scientific and technical facilities for the support from: Rumah Program Hasil Inovasi Teknologi Nuklir (HITN) 2023, with the decree of the Chairman of Research Organization for Nuclear Energy Number B-528/III.2/TN/2022, code D2475, and the Indonesia Endowment Fund for Education (LPDP) through a grant from the Research and Innovation for Indonesia Maju (RIIM) Batch 3 Number 12/II.7/HK/2023, code RIIM 29. Technical support from Nuclear, Chemical, and Physical Advanced Characterization Laboratories in the National Research and Innovation Agency through E-Layanan Sains-BRIN (ELSA-BRIN).

AUTHOR CONTRIBUTION

We confirmed that H. Sriwahyuni, Y. K. Krisnandi, T. Basuki, B. Setiawan, N. S. Pamungkas, and G. Nurliati are equal as the main contributors. The contributions of all authors are detailed below: H. Sriwahyuni: Conceptualization, Methodology, Validation, Formal analysis, Investigation, Writing original draft, Data curation, Writing review & editing, and Visualization. Y. K. Krisnandi: Conceptualization, Methodology, Validation, Formal analysis, Investigation, Writing review & editing, and Supervision. T. Basuki: Conceptualization, Methodology, Validation, Formal Analysis, Investigation, Writing review & editing, and Supervision. B. Setiawan: Conceptualization, Methodology, Validation, Formal Analysis, Investigation, Writing review & editing, and Supervision. A. Budiyanti: Formal Analysis, Validation, Writing review & editing, and Supervision. Z. Anggraini: Validation, Formal Analysis, Writing review & editing. N. S. Pamungkas: Data Curation, Visualization, Validation, Formal Analysis, Writing review & editing, and Supervision. All authors read and approved the final version of the paper. G. Nurliati: Validation, Visualization, Formal Analysis, and Writing review & editing.

REFERENCES

1. L. M. Krall, A. M. Macfarlane, and R. C. Ewing, Proc. Natl. Acad. Sci. U. S. A. **119** (2022) 1.
2. R. Sumarbagiono, P. A. Artiani, P. Basuki *et al.,* Nucl. Eng. Des. **426** (2024) 113373.
3. R. Kaushal, Rohit, and A. K. Dhaka, Biomass Convers. Biorefin. **14** (2024) 1427.
4. B. H. Shabalin, K. K. Yaroshenko, and S. P. Bugera, Nucl. Power Environ. **21** (2021) 78.
5. D. Deng, L. Zhang, M. Dong *et al.,* Water Environ. Res. **92** (2020) 1818.
6. A. Mishra and R. Khanal, Atom Indones. **49** (2023) 109.
7. B. Setiawan, D. Iskandar, G. Nurliati *et al.,* Atom Indones. **47** (2021) 65.
8. A. Shchipalkina and E. Smirnova, E3S Web Conf. **431** (2023) 1.
9. A. Asahara, D. Kawasaki, and S. Yanagihara, Nucl. Eng. Des. **374** (2021) 111066.
10. Muslim, H. Suseno, and M. J. Pratiwi, Atom Indones. **43** (2017) 41.
11. W. R. Prihatiningsih, H. Suseno, N. P. Zamani, *et al.,* Atom Indones. **42** (2016) 129.
12. Syarbaini, Kusdiana, and M. Wiyono, Atom Indones. **46** (2020) 99.
13. World Nuclear Association, Storage and Disposal of Radioactive Waste, https://world-nuclear.org/information-library/nuclear-fuel-cycle/nuclear-waste/storage-and-disposal-of-radioactive-waste. Retrieved in February (2025).
14. U. Bergström, K. Pers, and Y. Almén, International Perspective on Repositories for Low Level Waste, SKB R-11-16, Swedish Nuclear Fuel and Waste Management Co, Stockholm (2011) 78.
15. S. Kimura, K. Kitayama, H. Takahashi *et al.,* E3S Web Conf. **43** (2018) 4.
16. P. Delage, Y. J. Cui, and A. Tang, J. Rock Mech. Geotech. Eng. **2** (2010) 111.
17. G. Armand and J. Shao, Rock Mech. Rock Eng. **57** (2024) 4131.
18. R. Lenhard, R. Fedors, C. Manepally *et al.,* Buffer and Backfill Workshop Report, U.S. Nuclear Regulatory Commission, Contract NRC-02-07-006 (2011).

19. R. Pusch, Technical Report: The Buffer and Backfill Handbook, No. TR-02-12, Swedish Nuclear Fuel and Waste Management Co, Stockholm (2001) 1.
20. K. Ruan, H. Wang, H. Komine *et al.,* Soils Found. **62** (2022) 101245.
21. P. Herold, *Engineered Barrier Systems: Multi Barrier Systems in Geological Disposal*, European Joint Programme on Radioactive Waste Management (2020) 1.
22. M. Nazir, K. Kawamoto, and T. Sakaki, Int. J. GEOMATE **20** (2021) 132.
23. V. V. Krupskaya, S. V. Zakusin, V. A. Lekhov *et al.,* Radioact. Waste **10** (2020) 28.
24. B. Setiawan and H. Suseno, Eksplorium **38** (2017) 1.
25. H. Poernomo, Indones. J. Chem. **10** (2010) 276.
26. R. Mirkhani, M. H. Roozitalab, N. Khaleghpanah *et al.,* J. Radioanal. Nucl. Chem. **293** (2012) 587.
27. B. G. Shabalin, K. K. Yaroshenko, S. P. Bugera, Nucl. Power Env. **2** (2021) 78.
28. P. Belousov, A. Semenkova, T. Egorova *et al.,* Miner. **9** (2019) 1.
29. Sucipta and D. Suganda, IOP Conf. Ser. Mater. Sci. Eng. **432** (2018) 012027.
30. S. De Gisi, G. Lofrano, M. Grassi *et al.,* Sustainable Mater. Technol. **9** (2016) 10.
31. Z. Rahal, A. Khechekhouche, A. Barkat *et al.,* Indones. J. Sci. Technol. **8** (2023) 397.
32. H. F. D. Supratman, H. A. Pratama, B. Setiawan *et al.,* Environ. Chem. Ecotoxicol. **7** (2025) 252.
33. M. Yusuf, AIP Conf. Proc. **2374** (2021) 020017-1.
34. M. Yusuf and D. S. Wisnubroto, AIP Conf. Proc. **2967** (2024).
35. S. P. Santoso, A. Kurniawan, A. E. Angkawijaya *et al.,* Chem. Eng. J. **452** (2023) 139261.
36. N. Yaghmaeiyan, M. Mirzaei, and R. Delghavi, Results Chem. **4** (2022) 100549.
37. M. M. Marintan, F. Sjatha, D. A. Nurani *et al.,* Sci. Technol. Indones. **9** (2024) 325.
38. R. Hatel, S. El Majdoub, A. Bakour *et al.,* IOP Conf. Ser.: J. Phys. **1081** (2018) 012006.
39. A. Yuliyanti, A. T. Mursito, W. Widodo, S. R. Muharam *et al.,* Riset Geologi dan Pertambangan **28** (2018) 13. (in Indonesian)
40. T. Al-Ani and O. Sarapää, Geological Survey of Finland: Clay and Clay Mineralogy, Geologian Tutkuskeskus M19/3232/2008/41, Espoo (2008) 1.
41. G. E. Christidis, Appl. Clay Sci. **13** (1998) 79.
42. Z. A. Alothman, Mater. **5** (2012) 2874.
43. N. S. Pamungkas, D. Wongsawaeng, D. Swantomo *et al.,* Atom Indones. **50** (2024) 165.
44. N. S. Pamungkas, D. Wongsawaeng, D. Swantomo *et al.,* Eng. J. **27** (2023) 45.
45. X. Wang, H. Cheng, P. Chai *et al.,* Energy and Fuels **34** (2020) 12204.
46. P. Lawtae and C. Tangsathitkulchai, Mol. **26** (2021) 6521.
47. A. Fisli, Sumardjo, and Mujinem, Indones. J. Mater. Sci. **10** (2008) 12.
48. P. Aim-O, N. S. Pamungkas, S. Nawong *et al.,* J. Phys. Conf. Ser. **2431** (2023) 012069.
49. K. L. N. P. Aguiar, K. A. B. Pereira, M. S. L. Mendes *et al.,* J. Pet. Sci. Eng. **195** (2020) 107600.
50. G. Jozanikohan and M. N. Abarghooei, J. Pet. Explor. Prod. Technol. **12** (2022) 2093.
51. D. Gandhi, R. Bandyopadhyay, and B. Soni, Mater. Today Proc. **57** (2022) 194.
52. F. G. Alabarse, R. V. Conceição, N. M. Balzaretti *et al.,* Appl. Clay Sci. **51** (2011) 202.
53. R. Et-tanteny, B. El Amrani, and M. Benhamou, Chem. Phys. Impact **8** (2024) 100611.
54. A. M. Emara, E. M. Elsharma, and I. M. Abdelmonem, Radiat. Phys. Chem. **208** (2023) 110892.
55. Q. Zhang, Y. Zhao, L. Qin *et al.,* J. Radioanal. Nucl. Chem. **333** (2024) 5347.
56. M. Y. Prajitno, D. Harbottle, N. Hondow *et al.,* J. Environ. Chem. Eng. **8** (2020) 102991.
57. W. A. Muslim, T. M. Albayati, and S. K. Al-Nasri, Sci. Rep. **12** (2022) 1.
58. J. Y. Goo, B. J. Kim, J. S. Kwon *et al.,* Appl. Clay Sci. **245** (2023) 107141.
59. M. Ghaly, M. R. Abass, and Z. A. Mekawy, Environ. Sci. Pollut. Res. **30** (2023) 60432.
60. B. Setiawan, U. Zhafirah, and A. Saefumillah, Atom Indones. **45** (2019) 1.
61. S. Sarah, Baharuddin, Bustan, J. Soil Qual. Manage. **3** (2024) 1.